DIRECT GRAY SCALE RIDGE RECONSTRUCTION IN FINGERPRINT IMAGES

A Thesis Presented

by

Carlotta Domeniconi

to

International Institute for Advanced Scientific Studies

in Partial Fulfillment of the Requirements

for the Degree of

Master

in the field of

Information and Communication Advanced Technologies

International Institute Advanced Scientific Studies

Salerno, Italy

November 1997

Abstract

Automated identification of fingerprints is a difficult problem with many important applications. For the purpose of automation, a suitable representation (feature extraction) of fingerprints is essential. Most fingerprint recognition algorithms are typically based on extraction of certain feature points called *minutiae points*.

Several approaches have been proposed in the literature; although rather different from each other, all these methods transform fingerprint images into binary images. Nevertheless, all attempts to address feature extraction from fingerprint images through binarization seem to perform poorly on noisy images with low-contrast. This difficulty is strictly related to the binarization process itself: it causes a loss of a significant amount of information, which becomes crucial when the image has low-contrast. Moreover, the binarization phase is computationally expensive, it involves critical thresholds whose values are difficult to be set, and critically rely on a pre-processing phase.

In order to achieve more accurate results we perform an original technique which avoids binarization and thinning processes. Referring to the tools of differential geometry, we elaborate a fingerprint representation performing ridge point detection directly on gray scale images. Our basic idea is to view ridge lines as a sequence of maximum and saddle points.

The approach we describe does not make any use of critical threshold values and it does not critically rely on a pre-processing phase. The ridge point detection technique, together with the ridge reconstruction algorithm we implement, result in a

robust method which performs well on noisy ink detected images. It deals nicely, in fact, with over-inked areas and with breaks in ridges created by under-inked areas. The overall method is efficient, easily computable, and therefore amenable to automated matching algorithms. The multistage and computationally expensive approaches which perform binarization of the gray scale images, involving both segmentation and local thresholding phases, are avoided. Each step of our method can be hardware implemented, allowing a relevant speed up of the whole feature extraction process.

To my parents Francesca e Giorgio

Acknowledgements

This thesis has been possible thanks to many people who gave their supports in different ways. My stay at the University of California, in Riverside, gave me the opportunity to meet many interesting people and make new friends.

I first want to thank my advisor Prof. Ping Liang who actually made this opportunity possible, accepting to work with me during the development of the thesis. I enjoyed every discussions we had; I believe I have learned a lot from his insightful explanations and good ideas. It has been a pleasure working with him, and the chance of knowing him had a main influence for me to decide of pursuing my Ph.D. studies at UCR. Dr. Sibel Tari significantly contributed to many ideas presented in this thesis. Thanks to her I became familiar with many concepts of Computer Vision. I always seeked her advice whenever I felt lost, and she was always available for listening. I deeply appreciate her support and help, also for practical issues. I want to thank Dr. Hyung Jun Kim for discussions on wavelets and suggestions during the first phase of the work. I thank Boaz Yeger, system manager of the laboratory. He helped me many times with technical problems and he has been very patient with all my askings. I thank him for being very friendly and cheerful.

Back to Italy, many people contributed to this thesis. My family always supported me in pursuing my objectives. A special thanks goes to my friend Anna. We have shared many experiences during these years, both difficult and wonderful times. She became one of my best friends, and I think she will always be. Finally I want to say thanks to Marco, but no words really help. Even far away, he was always with me, through each phase of the work. He is a wonderful listener and a wonderful person to talk to. I consider my relationship with him a precious privilege, something I will always keep with me.

Contents

List of Figures

Chapter 1

Introduction

1.1 Introduction to Fingerprints

The term print or fingerprint refers to the impression of a finger retained on a surface after the finger is removed. The inner surface of a finger is covered with a pattern of friction ridges whose complexity renders each fingerprint unique. Impressions of these patterns can be recorded by applying a thin layer of ink to each finger and then pressing each finger onto a piece of paper. Even without ink, sweat pores along the top of the friction ridges may result in the inadvertent transfer of body oils to a receptive surface, creating an invisible impression of the fingerprint pattern. These invisible impressions are referred to as *latent* (meaning *hidden*) prints and can sometimes be made visible by the application of chemicals or powders that react with the deposits from the sweat pores in a different way than with the surrounding material.

Most fingerprint recognition algorithms are typically based on extraction of certain feature points called *minutiae points* [7]. As shown in Figure 1.1, a minutiae point is defined as the location where a single ridge bifurcates (splits) into two ridges or where

a ridge ends. The term *matching*, when used in the context of court evidence, includes such considerations as having identical minutiae point relative locations within the ridge structure, the ridge flow at corresponding minutiae being similar, the minutiae being of the same type (bifurcation or ridge ending), and the relative uniqueness of the features and their relationships. In U.S. courts of law, the matching of 12 minutiae is routinely accepted as evidence of identification.

Figure 1.1: Example of minutiae points: bifurcation and end points are highlighted.

Other features besides minutiae points are frequently used to classify fingerprints so they can be filed for future retrieval [13]. The most important of these additional features are the *type lines* (which enclose the area of a fingerprint used to determine its classification), the *delta*(s), and the *core*. Type lines are the two innermost ridges which start parallel, diverge, and surround or tend to surround the pattern area. The delta is the point on a ridge at or in front of and nearest to the center of

the divergence of the type lines. The core is the approximate center of the finger impression, and is always placed on or within the innermost ridge with *sufficient recurve*. A greatly oversimplified definition of a ridge with sufficient recurve is that the ridge doubles back on itself and does not intersect any other ridges near the loop. If these definitions of type lines, deltas, and cores sound imprecise or difficult to apply, it is because in many cases they are. The Department of Justice handbook, The Science of Fingerprints, presents dozens of rules and examples for determining these features in a variety of situations [7]. Therefore, automated classification of fingerprint types based on these rules is difficult to achieve. Using the above features, fingerprints can be categorized into three general classes, each of which can be further partitioned into a total of eight classes/subclasses, as shown in Figure 1.2. Further class subdivisions are also possible. As with the underlying feature data (e.g. minutiae, core, delta), fingerprint classification patterns are defined by a lengthy series of rules: the Science of Fingerprints devotes over 100 pages (half of the handbook) to the topic of fingerprint classification. Fingerprint classification is not a straightforward task, even for humans: some prints exhibit transitional behavior (i.e., they have characteristics of two or more patterns) and an element of subjective interpretation comes into play. Information may be missing from the fingerprint due to incomplete or imperfect recording of the friction ridge area. In this case fingerprint technicians must have allowances for all pattern types which might apply.

The motivation for partitioning and organizing fingerprint data into classes and subclasses is to avoid, where possible, having to search the entire database to determine if it contains a match to the inquiry print. The trade-off for this reduced search time is increased complexity, higher labor costs, and an increased possibility of errors related to misclassification of fingerprints.

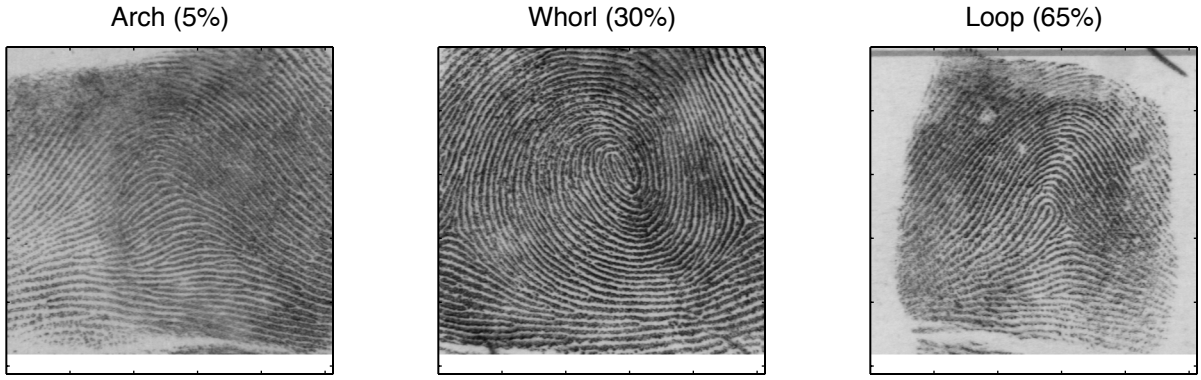

Figure 1.2: Major fingerprint classes. Arches can be further partitioned in Plain Arches and Tented Arches. Whorls can be partitioned in Plain Whorls, Accidental Whorls, Double Loop Whorls, and Central Pocket Loop Whorls. Loops can be partitioned in Ulnar and Radial.

Automated classification of fingerprints into four or five high-level pattern classes can achieve an accuracy of 95 to 99%. This accuracy can be achieved only if rejection of as many as 10 to 20% of the input prints is allowed which then must be treated as unknown or classified by a human. A second level of automated classification takes into account information such as the ridge counts between cores and deltas and is both time consuming and prone to errors. At the third level, features such as minutiae locations, types, and orientations are extracted. Then, all fingerprints with the same classification are searched for a match with the input fingerprint. This step is called the *print-to-print search*, i.e., search for a matching of fingerprints to determine if they come from the same finger of an individual. The print-to-print search compares features extracted from the input fingerprint image with features extracted from fingerprint images in the database. A typical fingerprint may contain between 70 to 100 minutiae points, and it may be positioned, rotated, and distorted differently than a matching database fingerprint, making print-to-print match a difficult and time con-

suming task. In the current state of the art of Automatic Fingerprint Identification System (AFIS), the matching algorithm must compute alternative matching scores for an extremely large number of relative orientations and correspondence between minutiae. A fingerprint image is rotated in small increment, say 0.5 degree, over a wide range, and matched to fingerprint images in the database. This is a very time consuming process; therefore further research to improve the print-to-print search response time and accuracy of AFIS is needed.

1.2 The History and Development of Fingerprinting

It is worth introducing at this point the major phases which belong to the interesting history and development of fingerprinting [15]. The story of the development and use of fingerprints in the last hundred years will only be properly appreciated with some knowledge of dactyloscopy, the science which studies patterns of ridges present on surfaces of the hands and of the feet. Therefore I will first briefly outline the basic details of this science.

The inside surfaces of the hands from fingertips to wrist and the bottom surfaces of the feet from the tip of the big toe to the rear of the heel contain minute ridges of skin, with valleys between each ridge. A cross section of a finger would look exactly like the cross section of a plowed field. Whereas on a plowed field the ridges and valleys run in straight parallel lines, on the hands and feet the ridges and valleys frequently curve and, especially on the fingertips and toe ends, the ridges and valleys form complicated patterns. The ridges have pores along their entire length that exude perspiration; hence, when an article is picked up, the perspiration runs along

the ridges and leaves an exact impression of them, just as an inked rubber stamp leaves its impression on a blank sheet of paper.

Ridges and valleys have evolved on the hands and feet to fulfill three specific functions:

1. Exudation of perspiration
2. Tactile facility
3. Provision of a gripping surface

The ridges and valleys form some basic characteristics. As already mentioned, some authorities consider that only two types of characteristics are present, a ridge ending and a bifurcation, all other characteristics being variations of the two basic forms.

The ridges and valleys form patterns on the last joint of the fingers and toes, forming three basic types: arches, loops, and whorls. There are variations of these patterns, especially with whorls. Every person in the world shares these patterns - a person can have all of one type, or even a mixture of all of them. The everyday use of fingers as an identification method and the production of finger and palm evidence in courts of law are based on one magnificent premise: no one has ever been found who has a sequence of ridge detail on the hands and feet that is identical to the ridge detail of any other person.

One of the earliest evidence of ridge detail on the hands and feet of humans was seen in the 4,000-year-old mummies of ancient Egypt. The hands and feet of mummies have been examined on numerous occasions, and the presence of ridge details on the mummies' digits is confirmed. In 1977, the mummy Asru, from the Temple of Karnak, was fingerprinted by experts in Manchester under the direction of Detective Chief Inspector Thomas Fletcher, head of the Fingerprint Bureau of the Greater Manchester Police. Mr. Fletcher used his experience as a detective to discover the

occupation of Asru in the Temple of Karnak; she was either a dancer or a chantress:

Three thousand years ago Egyptian temple dancers performed their ritual dances barefoot, the foot being used as part of the body's expression. The sole was in constant contact with the ground and even on the smoothest of flooring there would be friction and consequent wearing of the ridges on the underside of the toes and balls of the feet. Asru's feet did not show any traces of this constant contact with the floor, the depth of the furrows and the clarity of the characteristics were not consistent with her having been a dancer, and the alternative of her being a chantress was much more acceptable.

Another evidence reported was the presence of a small portion of palm imprint on hardened mud found in Egypt on a paleolithic site at the Sebekian deposit, Kom Ombo plain, on the east bank of the river Nile, dated around 10,000 years ago. The fact that primates have ridge detail was announced for the first time by Jan Evangelista Purkinje in his thesis published on December 22, 1823. He wrote:

In the hands of the monkeys, as well as in their prehensile tails, similar lines occur the distinction of which adds to the knowledge of the characteristics of all species. Zoologist, unless they consider them unimportant, will add further details.

In 1975-76, John Berry and his colleagues in the Fingerprint Office in Hertfordshire, U.K., commenced protracted research to confirm that all species of primates have ridges detail on their hands and feet in patterns and toe ends that conform to human patterns. They found out that, although Madagascan primates differ physically from African primates, they both bore ridge detail on their hands and feet. The most accredited theory which can account for this phenomenon states that ridge details

appeared on the hands and feet of our subprimate ancestors over 100,000,000 years ago, before the separation of Madagascar from the East African coast, and that our subprimate ancestors developed ridge detail on their hands and feet to facilitate the evolutionary requirement for grip, tactile facility, and the exudation of perspiration.

The earliest trace of finger imprints being purposely impressed occured in Mesopotamia and dates from circa 3,000 B.C. where an authority asserts that a "digital impression" was placed on each brick used in the construction of the king's storehouse. This method of making identifying marks is also found on bricks used in the construction of the "royal buildings" in Ancient Egypt. It is pertinent to note that in these two examples the buildings were for kings or pharaohs, suggesting the importance placed in the craftsmanship which was confirmed by the finger impressions of the masons.

A Chinese clay seal, dated before the third century B.C., has been the focus of considerable research and speculation for many years. A left thumb imprint is deeply embedded in the seal, and on the reverse side is ancient Chinese script representing the name of the person who made the thumb imprint. The mark is so specific in pressure and placing that there can be no doubt that it was meant as an identifying mark. If this is so, there is the strong inference that the Chinese were aware of the individuality of fingerprints well over 5,000 years ago. There is no evidence to conclude that the ancient Chinese were aware of the individuality of fingerprints on a universal basis. But the care taken to impress the clay seals suggests that the persons utilizing this form of signature were aware that the design on their fingers or thumbs so applied constituted individuality. This must represent, even at its crudest level, the local recognition that the person who impressed a digit on a seal was permanently bound to the contents of the documents so certified.

The first person to study and describe ridges, valleys, and pores on the hand and

foot surfaces was English plant morphologist Nehemiah Grew, born in Warwickshire in 1641. He was the first fingerprint pioneer; besides writing on the subject, he also published extremely accurate drawings of finger patterns and areas of the palm.

Grew's contemporary, Marcello Malpighi (1628-94), also a plant morphologist, researched the functions of the human skin, and the "Malpighian layers" were named after him. He worked at the University of Bologna, Italy, and in his publication he mainly dealt with the skin, although he did briefly mentioned ridge detail. It is believed that Grew and Malpighi corresponded to a degree, but the differences in language were a frustration, strangely because Graw was more adept at Latin than the Italian.

Joannes Evangelista Purkinje was a Bohemian and part of his thesis, quoted earlier, dealt in considerable detail with the functions of ridges, furrows, and pores; additionally, he illustrated and described nine fingerprint patterns: one arch, one tented arch, two loops, and five types of whorl.

The major step forward in the use of fingerprints was a method of classification that enabled fingerprint forms bearing differing patterns to be placed in a certain order, thus enabling the search area to be minimized. If a classification system did not exist, and a person gave a wrong name, each set of fingerprint forms would have to be examined to discover the correct identity of the offender. Many countries in the world now use the "Henry System", named after Edward Henry. His system became operational at Scotland Yard in 1901. The FBI, with its huge collection of fingerprint forms uses the basic Henry system, amended to the FBI's requirements.

Francis Galton and William Herschel also worked out classification systems. Herschel was an important figure in fingerprint pioneering because he was the first person to confirm ridge persistency, which states that the formation of ridge detail that de-

velops on the hands and feet in the womb does not change, except as a result of serious injury to the digits or decomposition after death. This is the major requirement for a fingerprint system.

Dr. Henry Faulds (1843-1930), a medical missionary, became extremely interested in fingerprints during his mission in Japan, performing experiments which proved that ridges details are immutable. In one classical experiment, he removed the skin from the fingers of his patients after fingerprinting them; when the skin regrew on the fingertips he fingerprinted them once more, noting that the ridge detail was exactly the same as it was before the skin was removed. It is believed that Faulds was the first person to identify finger imprints at crime scenes. It is worth mentioning the amazing letter that Faulds sent to Charles Darwin on February 15, 1880, requesting his aid in obtaining the finger impressions of lemurs, anthropoids, etc., *with a view to throw light on human ancestry.* On April 7, 1880, Darwin replied to Faulds:

Dear Sir,
The subject to which you refer in your letter of February 15th seems to me a curious one, which may turn out interesting, but I am sorry to say that I am most unfortunately situated for offering you any assistance. I live in the country, and from weak health seldom see anyone. I will, however, forward your letter to Mr. F. Galton, who is the man most likely that I can think of to take up the subject and make further inquiries.

The letter was passed to Galton as promised, but he reposited it in the Anthropological Institute where it stayed until 1894. It was in 1888 that Galton commenced his enthusiastic foray into dactyloscopy. Initially he collected only thumb impressions,

but in 1890 he commenced to collect full sets of finger impressions. He worked out, as mentioned earlier, a fingerprint classification system. Francis Galton was a great fingerprint pioneer as well as a man of considerable talent in many other areas. However, British fingerprint experts do not use the expression "Galton Ridges", which is much in vogue in the United States.

1.3 Automatic Fingerprint Identification System (AFIS)

Automated identification of fingerprints is a difficult problem with many important applications. Many AFIS are already in use in law enforcement applications. However, the technology is still developing and there are still many unsolved research problems [14]. The Federal Bureau of Investigation (FBI) has invested hundreds of million dollars to develop the world largest AFIS with a goal of up to 63 million criminal fingerprint records stored on-line and up to 11 million civilian records stored off-line.

An even larger market for AFIS that is emerging regards the verification of identity in cases such as bank ATM machine access, building access, credit card verification, welfare payment, voter registration, and employee background check. Identification methods based on memory data such as personal identification numbers and passwords, and methods based on possession of personal magnetic cards are widely used at present. However, none of these methods offers a high level of security. There is always the risk of another person obtaining one's personal identification number or using one's card. AFIS offer a solution to this problem, since fingerprints uniquely identify a person and their features remain invariant with age.

An AFIS consists of various processing stages as shown in Figure 1.3. For the purpose of automation, a suitable representation (feature extraction) of fingerprints is essential. This representation should have the following desirable properties:

- Retain the discriminating power (uniquiness) of each fingerprint at several levels of resolution (detail).
- Easily computable.
- Amenable to automated matching algorithms.
- Stable and invariant to noise and distorsions.
- Efficient and compact representation.

The compactness property of representation often constrains its discriminating power. Clearly, the raw digital image of a fingerprint itself does not meet these representational requirements. Hence, high-level structural features are extracted from the image for the purpose of representation and matching.

Commercially available fingerprint identification systems typically use ridge bifurcations and ridge endings as features. Because of the large size of the fingerprint database and the noisy fingerprints encountered in practice, it is very difficult to achieve a reliable one-to-one matching in all the test cases. Therefore, the commercial systems provide a ranked list of possible matches (usually the top ten matches) which are then verified by a human expert. Details of commercial fingerprint recognition systems from NEC, PRINTAK and MORPHO are in [15].

One of the main problems in extracting structural features is due to the presence of noise in the fingerprint image. Commonly used methods for taking fingerprint

impressions involve applying a uniform layer of ink on the finger and rolling the finger on paper. This cause the following types of problems:

- Over-inked areas of the finger create smudgy areas in the image.
- Breaks in ridges are created by under-inked areas.
- The skin being elastic in nature can change the positional characteristics of the fingerprint features depending upon the pressure being applied on the fingers.

Although inkless methods for taking fingerprint impressions are now available, these methods still suffer from the positional shifting caused by the skin elasticity. The noncooperative attitude of suspects or criminals also leads to smearing in parts of the fingerprint impressions. Thus a substantial amount of research reported in the literature on fingerprint identification is devoted to image enhancement techniques.

1.4 Fingerprint Representation

This work focuses on the fingerprint representation problem. The task is to achieve a suitable representation of fingerprints in order to efficiently solve the print-to-print matching problem. Each fingerprint is coded into a set of ridges structures, which retain the discriminating power of each fingerprint. We use an original technique based on ridge point detection directly from gray scale fingerprint images. Our method uses the tools of differential geometry [10, 16] and it is based on properties of the intensity surfaces of the gray scale fingerprint images, which are direct consequences of the nature of the fingerprint images themselves. The overall technique results in a robust and efficient algorithm.

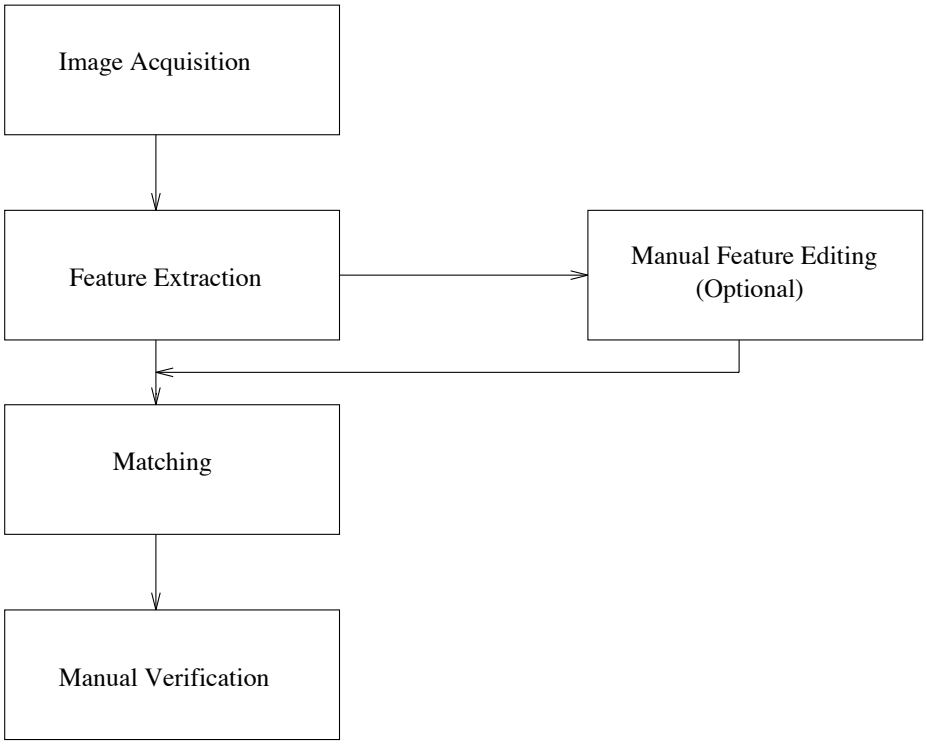

Figure 1.3: Stages in an AFIS.

The approach we describe does not make any use of critical threshold values, which are in general hard to be properly set. It does not critically rely on a pre-processing phase. We do perform a smoothing process prior to ridge point extraction but, since we do not attempt to perform binarization, degree of smoothing is not critical for our approach. Moreover, the ridge point detection technique, together with the ridge reconstruction algorithm we implement, result in a robust method which performs well on noisy ink detected images. It deals nicely, in fact, with over-inked areas and with breaks in ridges created by under-inked areas.

The overall method is efficient, easily computable, and therefore amenable to

automated matching algorithms. The multistage and computationally expensive approaches which perform binarization of the gray scale images, involving both segmentation and local thresholding phases, are avoided. Each step of our method can be hardware implemented, allowing a relevant speed up of the whole feature extraction process.

1.5 Organization of the Thesis

This thesis is divided into five chapters. Chapter 1 describes the features which make each fingerprint unique and distinguishable from each other, introduces Automatic Fingerprint Identification Systems, and in particular the feature extraction phase. Our approach to provide an adequate fingerprint representation is introduced and its advantages are highlighted. Next chapter briefly describes the techniques proposed in the literature. We point out how our method intends to overcome some limits and problems from which the techniques in the literature suffer. Information on data and experiments is also provided. Chapter 3 presents the ridge point detection technique. Concepts coming from differential geometry are described. Implementation and results are also discussed. Chapter 4 describes the ridge reconstruction algorithm. Enphasis is put on the purpose of the algorithm and on the strategies used to avoid the main problems algorithms which perform binarization have. Results are shown. Finally, chapter 5 discusses conclusions and future work.

Chapter 2

Background and Related Works

2.1 The Classical Approach

As already mentioned in chapter 1, automatic minutiae detection is an extremely critical process, especially in low-quality fingerprints where noise and low-contrast can originate pixel configurations similar to minutiae or hide real ones.

Several approaches have been proposed in the literature; although rather different from each other, all these methods transform fingerprint images into binary images [22, 21, 5, 19, 26, 17, 24]. Several intermediate steps are required. The overall process can be divided into three main operations: pre-processing and segmentation, binarization and thinning. The purpose of pre-processing is to apply a smoothing operation, which is quite critical since binarization is going to be performed. Segmentation is then applied to detect ridges. Usually some techniques for foreground and background contrast enhancement are then applied. Local thresholding is therefore performed in order to obtain a binary image, e.g. an image where the ridges have the value "1" (black) and the valleys have the value "0" (white) or vice versa. A thinning process

is applied on the binary image to obtain one pixel thick lines. Finally, a scan of the last image is able to detect the feature points.

The binarization phase is computationally expensive and it involves critical thresholds, whose values are difficult to be set. It may cause a loss of a significant amount of information, as it happens when a gray scale image is transformed into a binary image. As a consequence, when the gray scale fingerprint image is a low-quality image, the binary image presents configurations due to noise, which will cause false minutiae detection. Once the binary image is obtained, is very difficult to get rid of such configurations.

Also thinning the binary image is not an easy or trivial task. Many thinning algorithms have been proposed in the literature [2, 25, 12]. Various authors perform line thinning using line following [4], which seems to provide good results on fingerprints. It preserves, though, the noisy configurations of the binary image.

2.2 Our Attempt to Perform Binarization

We first addressed the feature extraction problem performing binarization and thinning processes on the fingerprint images. The results obtained, although comparable and sometimes of a better quality than the results published in the literature [19, 26, 17, 24], are still unsatisfactory for our purpose of solving the print-to-print matching problem.

We first applied a selective smoothing process which allows to preserve the ridges. We then performed edge detection using the Marr-Hildreth operator [11, 3]. Median filters are applied to the original gray scale image with boundaries superimposed, in order to enhance the background-foreground contrast. At this point, a sophisti-

cated local thresholding algorithm is applied to the enhanced image with boundaries superimposed. The image is scanned twice, both by rows and columns. A local thresholding technique, based on the comparison between averaged gray levels of adjacent areas separated by boundaries, is applied. Two binary images are the result of the horizontal and vertical scanning procedures. Combining these two binary images with the logical AND operator allows to erase some of the noise caused by lack of contrast in the gray scale image. We used the thinning procedure implemented in Matlab Version 5.1.0, and also implemented the skeletonization algorithm presented in [11] for a comparison.

2.3 A Different Point of View

The overall binarization procedure we implemented gives good results on fingerprint images with enough contrast. Noisy areas give rise to noisy skeleton areas, with pixel configurations which cause false minutiae detection (two obtained skeletons are shown in §4.3). An attempt to erase such configurations has been performed. Although cross-ridge noise causes pixel configurations which are visually distinctive, it is practically impossible to erase them performing local analysis, unless introducing false possible breaks.

All attempts to address feature extraction from fingerprint images through binarization seem to perform poorly on noisy images with low-constrast. This difficulty is strictly related to the binarization process itself: it causes a loss of a significant amount of information, which becomes crucial when the image has low-contrast.

In order to achieve more accurate results we perform a different technique which avoids binarization and thinning processes. Referring to the tools of differential ge-

ometry, we elaborate a fingerprint representation performing an analysis directly on gray scale fingerprint images. Our basic idea is to view ridge lines as a sequence of maximum and saddle points. The overall analysis results in a robust algorithm, since all mathematical properties used are direct consequences of the nature of the fingerprint images. Details of the techniques are described in chapters 3 and 4.

2.4 Data and Experiments

The National Institute of Standard and Technology makes available three databases of fingerprint images: NIST Special Database 4, NIST Special Database 9, and NIST Special Database 14 [27, 28, 29]. Nist Special Database 4 contains 2000 couples of 8-bit gray scale fingerprint images. Each couple corresponds to two different images, in terms of possible scales and orientations, of the same finger. Each image is 512×512 pixels with 32 rows of white space at the bottom of the print. The fingerprints are classified into one of five categories (L = left loop, W = whirl, R = right loop, T = tented arch, A = arch) with an equal number of prints from each class. The images have a NIST IHEAD raster format. Included with the images is a software to convert the images into sun raster format. We converted into sun raster format 50 sample images which belong to NIST Special Database 4. The images were then converted into TIF format. These images are used to test our algorithms. All experiments are implemented using Matlab Version 5.1.0. This work has been done at the Neural Networks and Pattern Recognition Research Laboratory, Electrical Engineering Department, University of California, Riverside, using a Ultra1 Sun Sparcstation.

Chapter 3

Detection of Ridge Points

3.1 Introduction

In this chapter we describe in details our technique for detecting ridge points directly from gray scale fingerprint images, and the correlated concepts of differential geometry.

Since fingerprint images may be very noisy, especially those acquired by ink technique like the ones we use in our experiments, it is appropriate to smooth the images prior to ridge point extraction. We smooth the image using geometric heat equation, by applying gradient descent to the functional [1, 23, 18]:

$$\int\int |\nabla I| dxdy.$$

Since we do not attempt to perform binarization, degree of smoothing is not extremely critical. Still we avoid using smoothing tools such as convolution with a Gaussian kernel which is equivalent to isotropic diffusion equation. Such non-selective smoothing tends to smear out the ridges. Geometric heat equation provides a good

enough smoothing while preserving the ridges, and it is invariant with respect to contrast.

3.2 Stationary Points

Let I be a $m \times n$ gray scale image with g gray levels, and $gray(i,j)$ be the gray level of pixel (i,j) of I, with $i = 1,...,m$, $j = 1,...,n$. Let $z = S(i,j)$ be the surface corresponding to the image I : $S(i,j) = gray(i,j)$, $i = 1,...,m$, $j = 1,...,n$. By associating bright pixels with gray levels near zero and dark pixels with gray levels near one, fingerprint ridge lines (appearing dark in I) correspond to intensity ridges, and spaces between ridge lines (appearing bright in I) correspond to intensity valleys (see Figure 3.1). From a mathematical point of view, ridge points are local maxima along the direction of one of the principal curvature and they are points where the other principal curvature is zero. An obvious way to detect ridge points is to examine the second derivatives. Let H denote the hessian matrix at a stationary point p. Let λ_1 and λ_2 , such that $|\lambda_1| \geq |\lambda_2|$, be the characteristic values of H, e.g. the roots of the characteristic polynomial $det(H - \lambda I)$ where the determinant is zero. Since the eigenvalue with the maximum absolute value corresponds to the direction along which intensities have maximum change, if p is a ridge point then

$$\lambda_1 < \lambda_2 = 0. \tag{3.1}$$

In real cases, detection of ridge points is not stable. Slight perturbations due to various factors (e.g. *noise, discretization grid size*) may change zero eigenvalues to non-zero values. A point which satisfies conditions (3.1) at a given resolution, may not satisfy the same conditions at a higher resolution. As a consequence, in general, our "ideal" ridges will change into a sequence of local maxima and saddle points (see

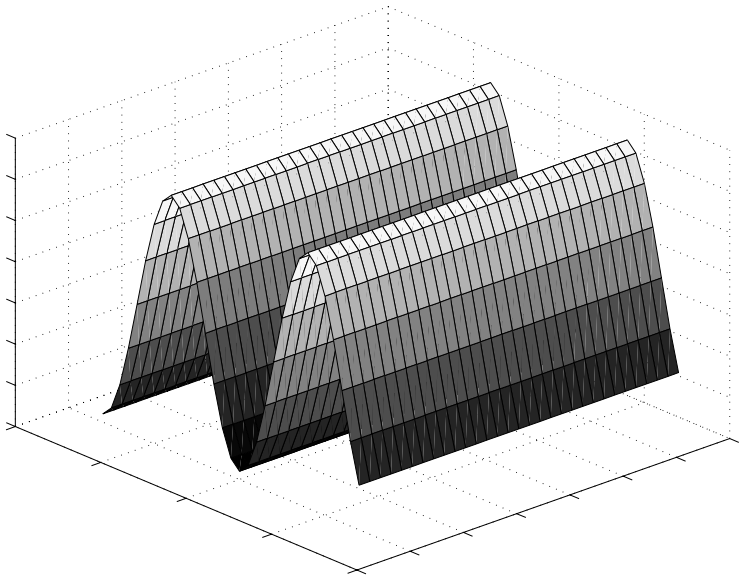

Figure 3.1: Ideal ridge surface.

Figure 3.2). Hence it is appropriate to search for such a general pattern rather than the idealized ridges of Figure 3.1.

A stationary point p is a local maximum iff

$$\lambda_1 \leq \lambda_2 < 0. \tag{3.2}$$

A stationary point p is a saddle point iff

$$\lambda_1 \lambda_2 < 0.$$

To distinguish saddle points which are on a ridge from the ones which are on a valley, we consider only the saddle points which are local maxima in the direction of maximum change and local minima in the direction of minimum change. Thus we establish that a stationary point p is a saddle point (on a ridge) iff

$$\lambda_1 < 0$$

$$\lambda_2 > 0. \tag{3.3}$$

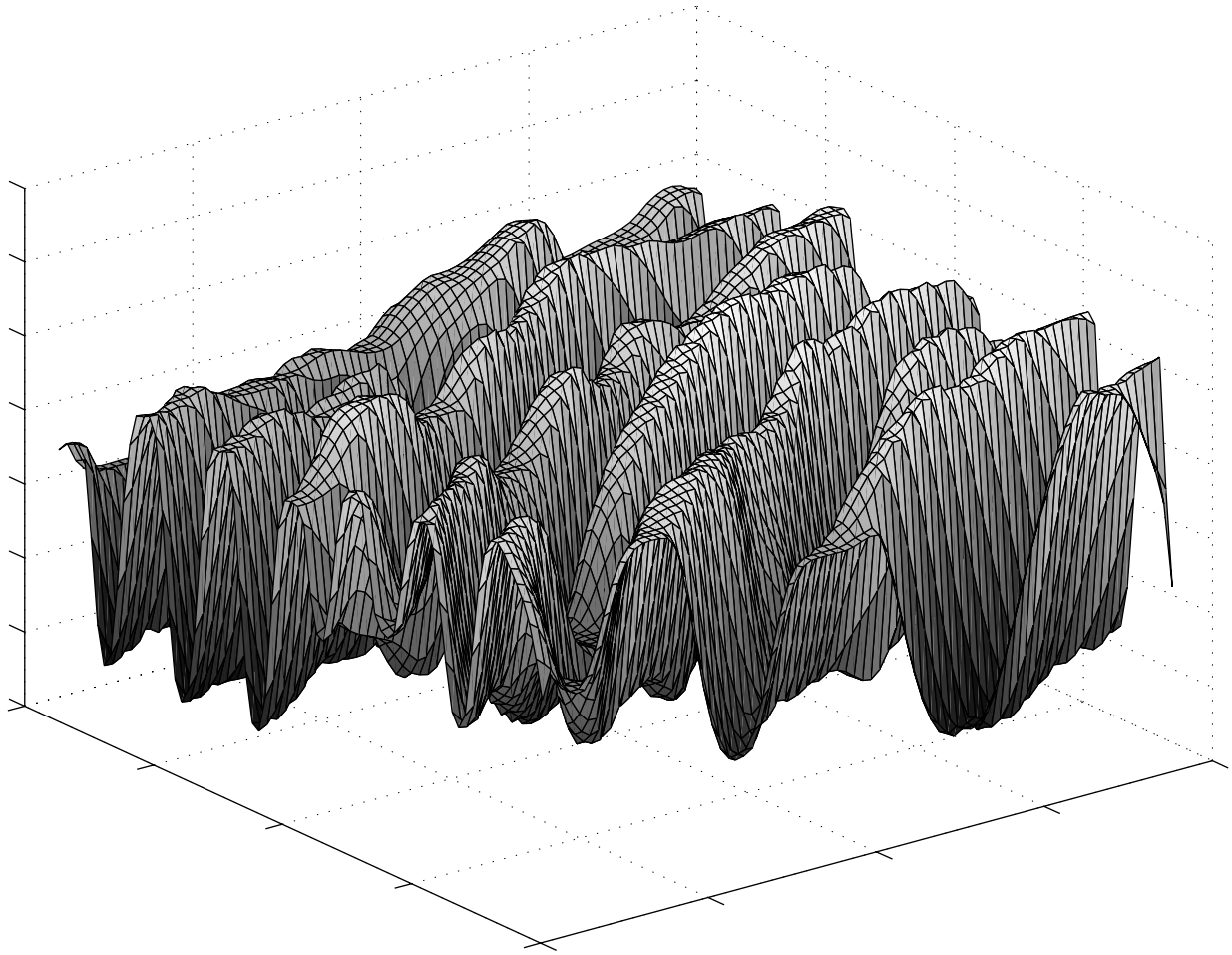

Figure 3.2: Surface corresponding to a small area of a fingerprint. It shows how our "ideal" ridges change into a sequence of local maxima and saddle points.

3.3 Implementation and First Results

Let $I_x = \frac{\partial I}{\partial x}$ and $I_y = \frac{\partial I}{\partial y}$ be the differences in intensity values in the x (column) direction and in the y (row) direction respectively. We detect the stationary points as the simultaneos zero-crossings of I_x and I_y. The zeros of I_x and I_y are located by scanning the two images I_x and I_y from top to bottom and from left to right to detect sign changes. For each pixel, if sign changes are detected during both scanning, the correspondent pixels are marked as stationary points in an output image. It is important do underline that detection of stationary points does not rely on the condition for the absolute value of the gradient vector (I_x, I_y) to be zero. Due to discretization factors and numerical gradient computation, in fact, the absolute value of the gradient vector may always have a positive value, and the use of a threshold on this value is not a robust and reliable technique. The hessian matrix H is computed at each stationary point using central differences. H is a 2×2 real symmetric matrix

$$H = \begin{pmatrix} I_{xx} & I_{xy} \\ I_{xy} & I_{yy} \end{pmatrix}$$

.

The roots of the characteristic polynomial $det(H - \lambda I)$, which is a second degree polynomial, give the eigenvalues. Once the eigenvalues are computed, maximum and saddle points are easily determined using (3.2) and (3.3).

Figure 3.3 and Figure 3.4 show the maximum and saddle points detected for two subimages of a fingerprint image (s02) belonging to NIST Special Database 4. Figure 3.5 shows the whole original fingerprint image. The two areas considered are highlighted. Figure 3.3 belongs to a rather clean area of the image in Figure 3.5; its resolution is 71×71 pixels. Figure 3.4 belongs instead to a very noisy area of the same image; its resolution is 130×110 pixels. Smoothing process has been applied prior

to ridge point detection in both cases. We do not distinguish between maximum and saddle points since for our ridge reconstruction purpose they have the same meaning.

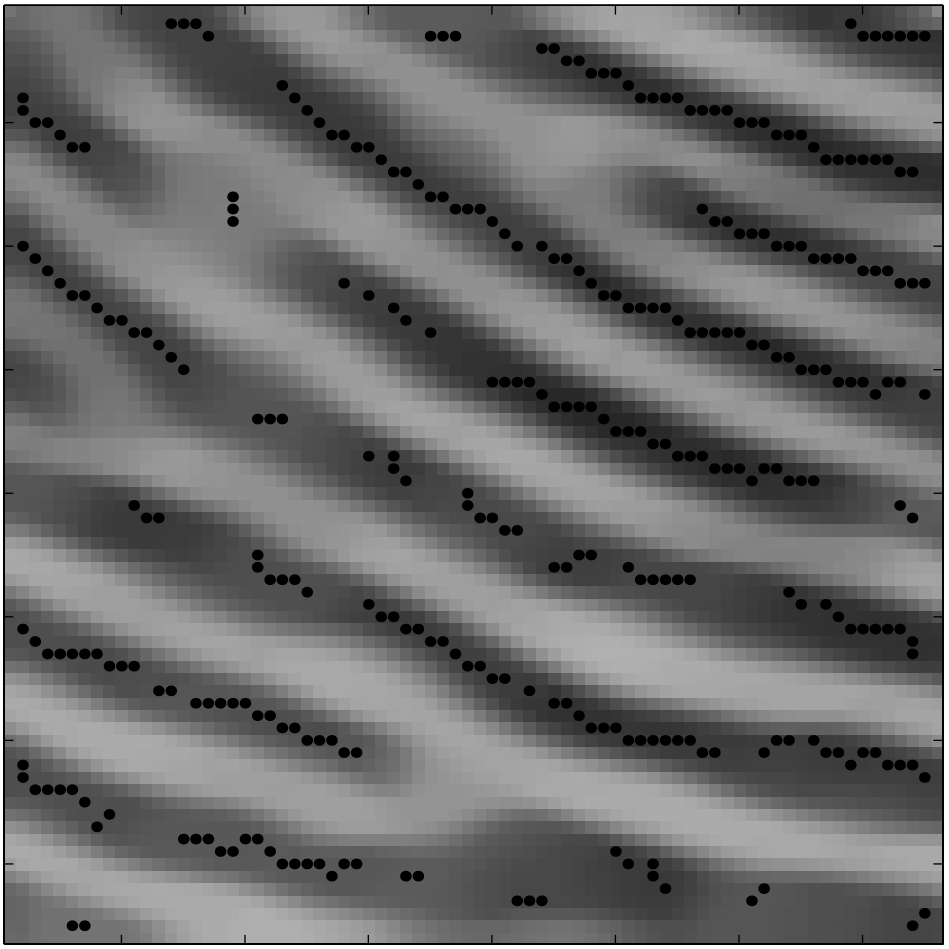

Figure 3.3: Results of maximum and saddle point detection on a clean area of a fingerprint image. Both maximum and saddle points are shown as back dots.

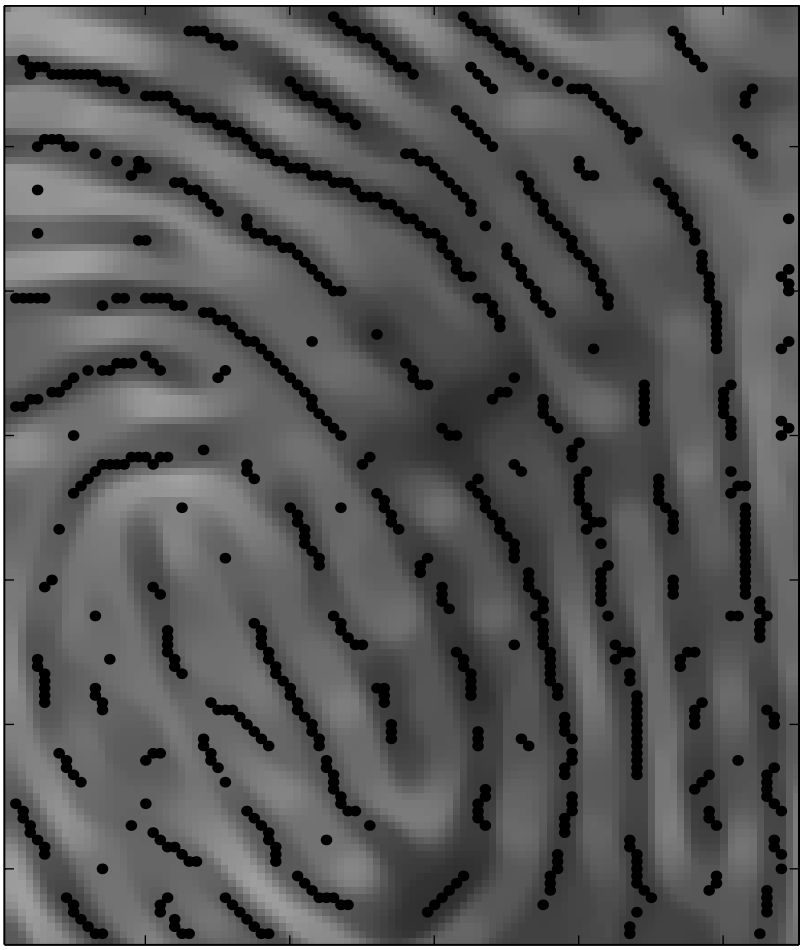

Figure 3.4: Results of maximum and saddle point detection on a noisy area of a fingerprint image. Both maximum and saddle points are shown as back dots.

Figure 3.5: Original fingerprint image. The two areas considered are highlighted with circles.

3.4 Gaps Between Stationary Points

Even though the maximum and saddle points shown in Figure 3.3 and in Figure 3.4 reliably belong to fingerprint ridges, there exist consistent gaps between them. Figure 3.2 explains why this phenomenon happens. Fingerprint ridge pixels may gradually change their intensity values along the ridge direction, causing branches of the ridge surface to have positive or negative slope. This phenomenon is evident near the ridges endings, as Figure 3.2 shows. Figure 3.6 shows the same phenomenon in the vicinity of a ridge along the ridge direction. Ridge's branches with positive or negative slope have no stationary points. Figure 3.7 shows the zero-crossings of the x and y gradient components I_x and I_y of the image in Figure 3.3. The intersection points between the two zero levels correspond to the simultaneous zero-crossings of I_x and I_y, hence to the stationary points. Some ridges show a behavior close to an "ideal" ridge; for those ridges the two curves run close to each other and often intersect. For some ridges, instead, the two curves present significant branches with no intersections; these branches correspond to the gaps between maximum and saddle points in Figure 3.3. Pixels on those ridge's branches are still maximum points along the orthogonal direction. Figure 3.8 shows the plot of the gradient vectors which correspond to the portion of the ridge shown in Figure 3.6. The branch of the ridge with no zero-crossing points is highlighted with a circle.

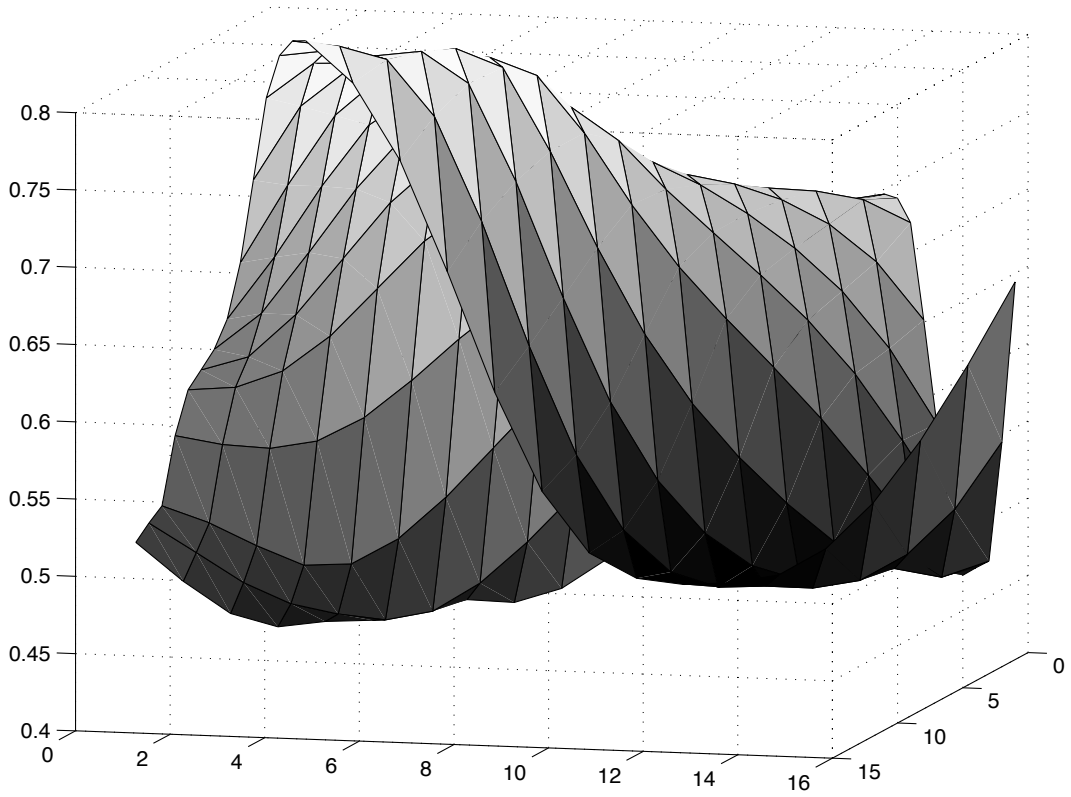

Figure 3.6: Surface of a portion of a fingerprint ridge.

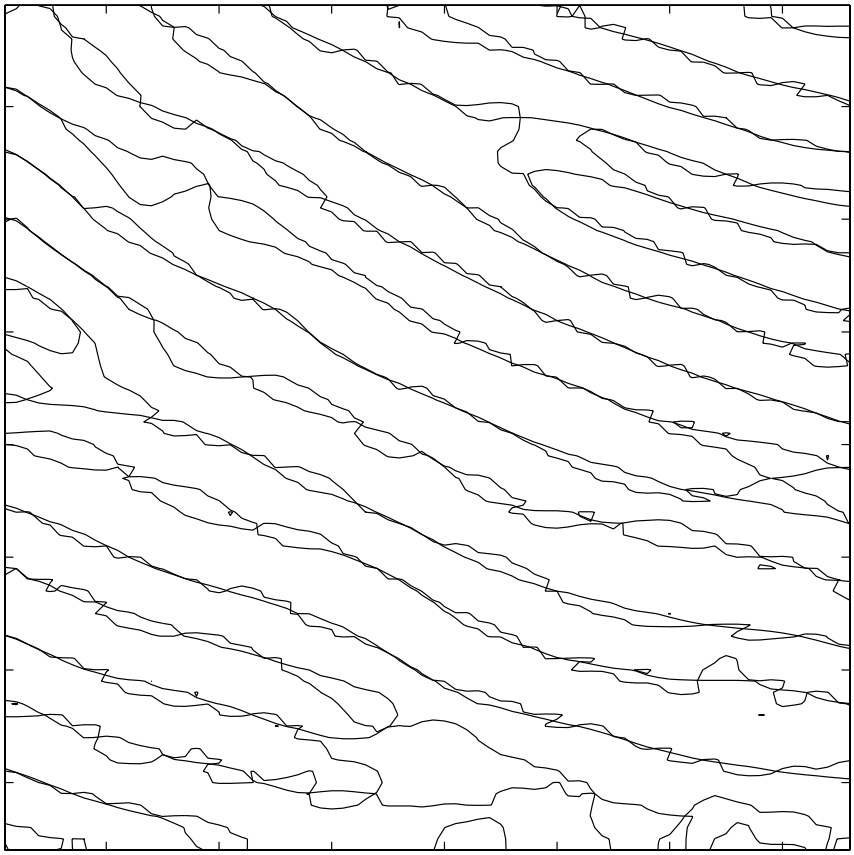

Figure 3.7: Zero-crossings of the x and y components of the gradient.

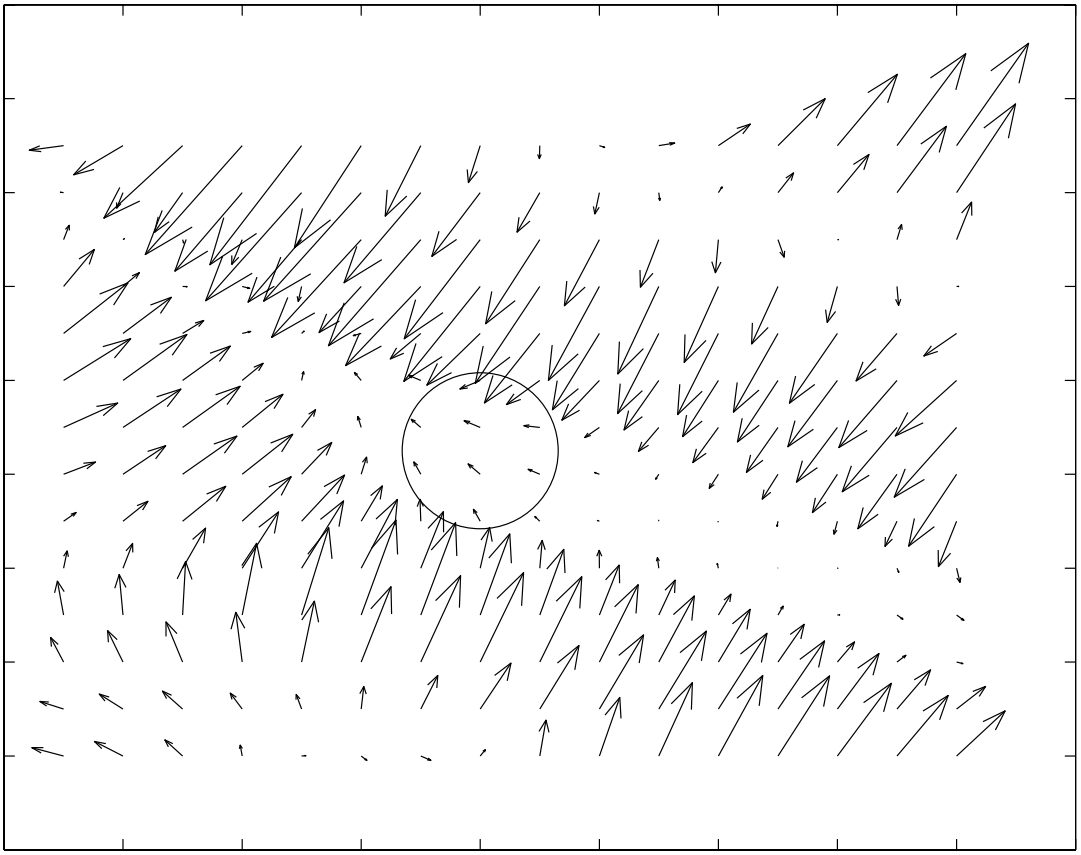

Figure 3.8: Gradient vectors corresponding to a portion of a ridge.

3.5 Non Stationary Points

Let p be a point on a ridge which is not a stationary point. Let p_1 and p_2 be the two neighbors of p along the direction orthogonal to the ridge. Let $\vec{n}_1$ and $\vec{n}_2$ denote the gradient vectors at pixels p_1 and p_2. Since p is a maximum point along the orthogonal direction, the gradient vectors $\vec{n}_1$ and $\vec{n}_2$ point at opposite directions:

$$\frac{\vec{n}_1}{|\vec{n}_1|} \cdot \frac{\vec{n}_2}{|\vec{n}_2|} = \cos(\pi) = -1 \tag{3.4}$$

This pattern is searched for non stationary points. For each non stationary point p, the four neighbor couples in the horizontal, vertical, and two diagonal directions are considered. A test is made to verify if condition (3.4) is satisfied for any of the neighbor couples in the four directions. If condition (3.4) is satisfied for at least one neighbor couple, the second derivatives at point p are investigated, in order to establish if it belongs to ridges or it belongs to valleys. Same criteria as in (3.2) and (3.3) are applied. A point p whose neighbors satisfy condition (3.4) is a ridge point situated on a negative slope iff condition (3.2) applies. A point p whose neighbors satisfy condition (3.4) is a ridge point situated on a positive slope iff condition (3.3) applies. In real cases equation (3.4) may never be satysfied due to the presence of noise. As a consequence, vectors $\vec{n}_1$ and $\vec{n}_2$ will have directions which are "almost" opposite.

It is important to underline that using the gradient direction for ridge detection is quite stable, whereas selecting ridge points by setting a threshold on the absolute value of the gradient is not a robust condition. This is because the appropriate threshold may change from image to image, or even from area to area within the same image. All our conditions are based on properties of the intensity surfaces of the gray scale images. Those properties are direct consequences of the nature of the

fingerprint images.

3.6 Results of Ridge Point Detection

Figure 3.9 and 3.10 show the stationary and non stationary points detected on the same images shown in Figure 3.3 and in Figure 3.4. In our experiments we use the value $\frac{5}{9}\pi$ for the angle between $\vec{n}_1$ and $\vec{n}_2$. Different values belonging to the interval $(\frac{\pi}{2}, \frac{2}{3}\pi]$ were tested. The results obtained have shown to be not particularly sensitive to the specific value used within the range considered.

Most of the gaps between stationary points shown in Figure 3.3 and Figure 3.4 are now recovered. A comparison between Figure 3.9 and Figure 3.3 clearly show how the detected non stationary points can trace with high precision the endings of ridges.

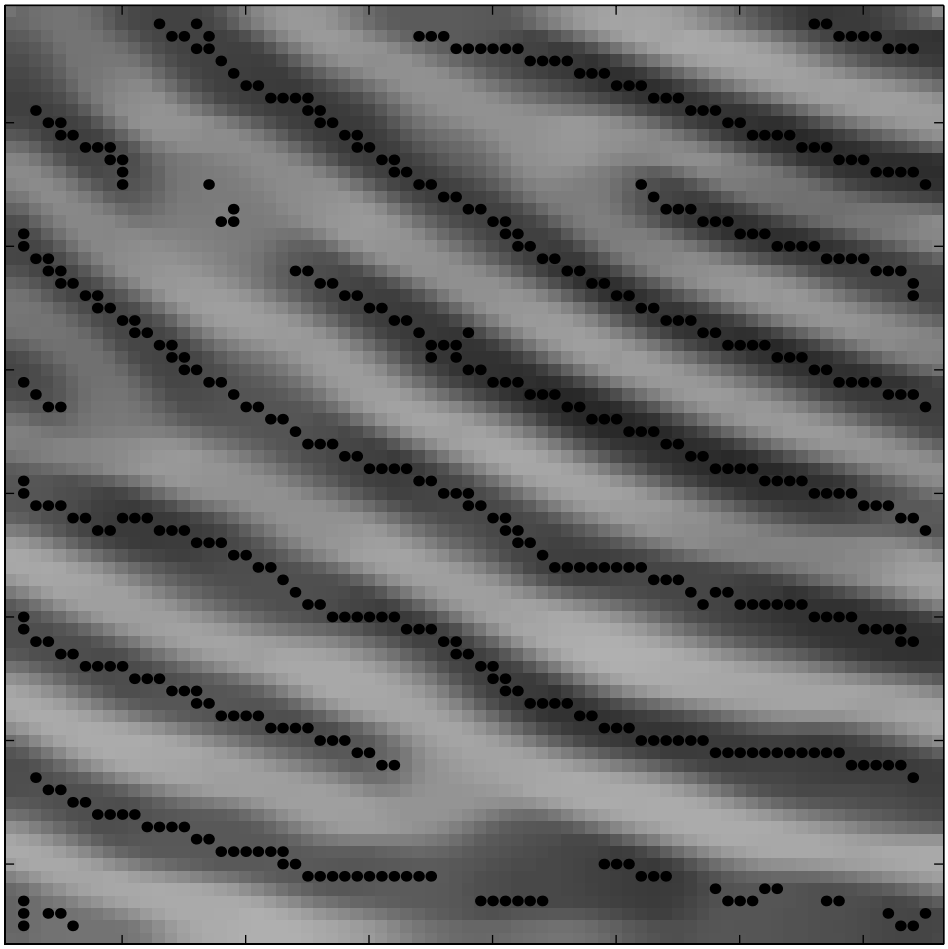

Figure 3.9: Results of stationary and non stationary points detection on a clean area of a fingerprint image. Both stationary and non stationary points are shown as black dots.

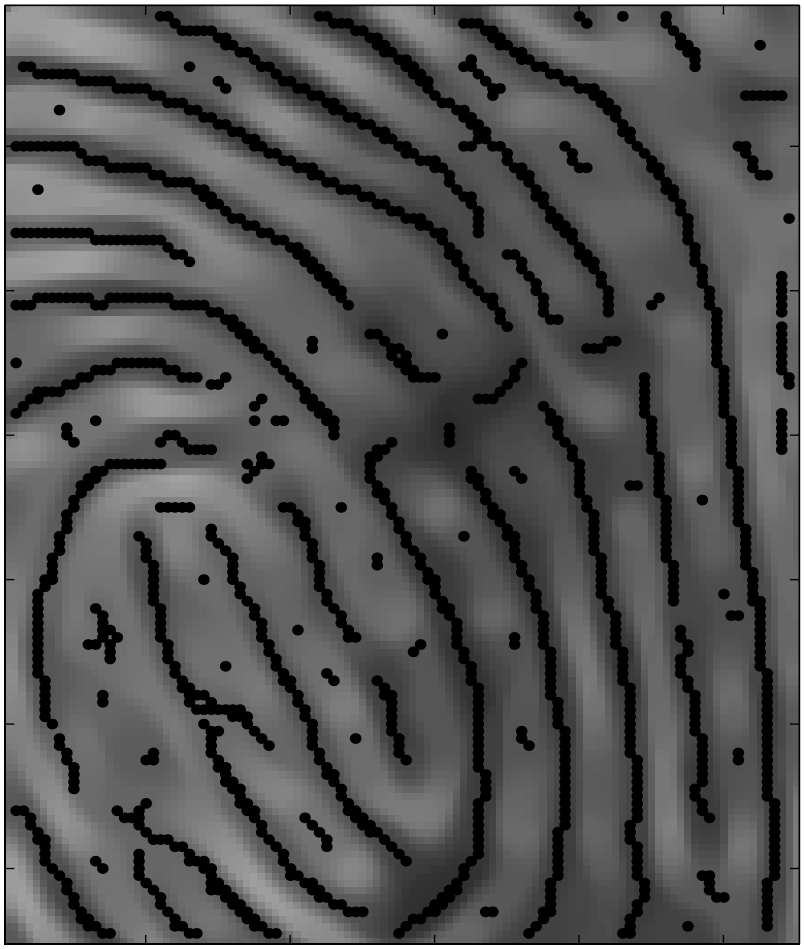

Figure 3.10: Results of stationary and non stationary points detection on a noisy area of a fingerprint image. Both stationary and non stationary points are shown as black dots.

Chapter 4

Reconstruction of Ridges

4.1 Purpose of Ridge Reconstruction

In chapter 3 an easy and robust technique for finding ridge points was presented. In this chapter we address how to use the ridge points to perform ridge reconstruction. The purpose of our ridge reconstruction algorithm is to collect and organize, in meaningful structures, the detected ridge points which are connected and to properly recover, if present, the gaps between them. The resulting structures correspond to our representation of fingerprint images which can be directly used to address the print-to-print matching problem. Our ridge reconstruction algorithm is completely driven by the points already detected. No ridge following algorithm based on gradient information is performed, since ridge points are available.

4.2 Ridge Reconstruction Algorithm

Each branch of connected points is traced only once starting from one of its end point. Once the opposite end point is reached, minimum squared error (mse) line fitting is

performed at both endings, to determine the directions along which move forward to look for other nearby branches. If a branch not traced yet is found, gap is filled with points and tracing of connected points continues; if a branch of a ridge already traced is encountered the gap is filled with points and the two branches are merged. When all branches of connected points are traced the algorithm stops. All merged branches belong to the same data structure which is stored in memory.

The pseudo-inverse approach is performed to implement *mse* line fitting [9]. Two parameters are involved in the *mse* line fitting procedure: the number of points to be used for computing the line equation and the number of pixels to move forward to look for a nearby branch. The first parameter has to have a value of at least four points. We do not allow gap filling, in fact, if the branch of connected points which has been traced is too short (less than four pixels in our experiments). A short ridge is kept isolated unless a merging with it takes place starting from a long enough branch. This technique allows to avoid false connections which can arise on account of the presence of noise across ridges. False connections due to the presence of noise across ridges are a serious problem of algorithms which perform binarization of fingerprint images. The specific value of the first parameter, as long as it is bigger than a minimum number of pixels, does not affect the results. In our experiments we use values of 10 and 20 pixels. The second parameter should not be bigger than the average distance between ridges in the image. Hence, appropriate values for both parameters can easily be found.

4.3 Results

The result of the ridge reconstruction algorithm applied on points shown in Figure 3.9 is shown in Figure 4.1. In this case 20 points or at least 4 points (if 20 points are not available on the branch which is currently traced) are used, when performing *mse* line fitting, and 4 pixels is the distance recovered along the tangent direction given by the *mse* line fitting. The result of ridge reconstruction for points shown in Figure 3.10 is shown in Figure 4.2. For this image 10 points are used when performing *mse* line fitting, and 6 pixels is the distance recovered along the tangent direction. The algorithm is able to recover most of the breaks between branches belonging to the same ridge. Moreover, the algorithm is able, almost always, to avoid false connections which can arise on account of the presence of noise across ridges. This result is particularly evident in Figure 4.2, which correspond to a noisy area of a fingerprint image. Most of the noise across ridges is kept isolated and false connections are avoided. Noise across ridges gives rise to short ridges of few pixels (two or three) which are stored in memory. These branches can be easily removed during a post processing phase. The improvement achieved performing ridge reconstruction directly from gray scale images can be easily appreciated comparing the result shown in Figure 4.2 with the skeleton obtained performing binarization of the same fingerprint image (see Figure 4.3). The local thresholding algorithm explained in §2.2 has been applied in order to obtain the skeleton showed. The area we performed ridge reconstruction on is highlighted with a circle. Many false connections are present within the circled area, due to the noise present in the original image. These false connections give rise to visually distinctive "H" shapes. Real fingerprints do not have such patterns. Although these configurations are visually distinctive, it is impossibile in practice to automatically erase them performing local analysis, unless introducing other false possible breaks.

Almost all these false connections are avoided in Figure 4.2.

Finally we want to show the result on a sample fingerprint image classified as a poor quality image [8]. The original fingerprint image, which belongs to NIST Special Database 4, is shown in Figure 4.4. Resolution is 271×271 pixels. The result of ridge point detection is shown in Figure 4.5. The result of ridge reconstruction is shown in Figure 4.6. In this case 20 points are used when performing *mse* line fitting, and 6 pixels is the distance recovered along the direction given by the *mse* line fitting. Once again the skeleton obtained performing binarization is shown in Figure 4.7 for a comparison. Again the false connections present in the skeleton are avoided when performing ridge point detection and ridge reconstruction directly from the gray scale image.

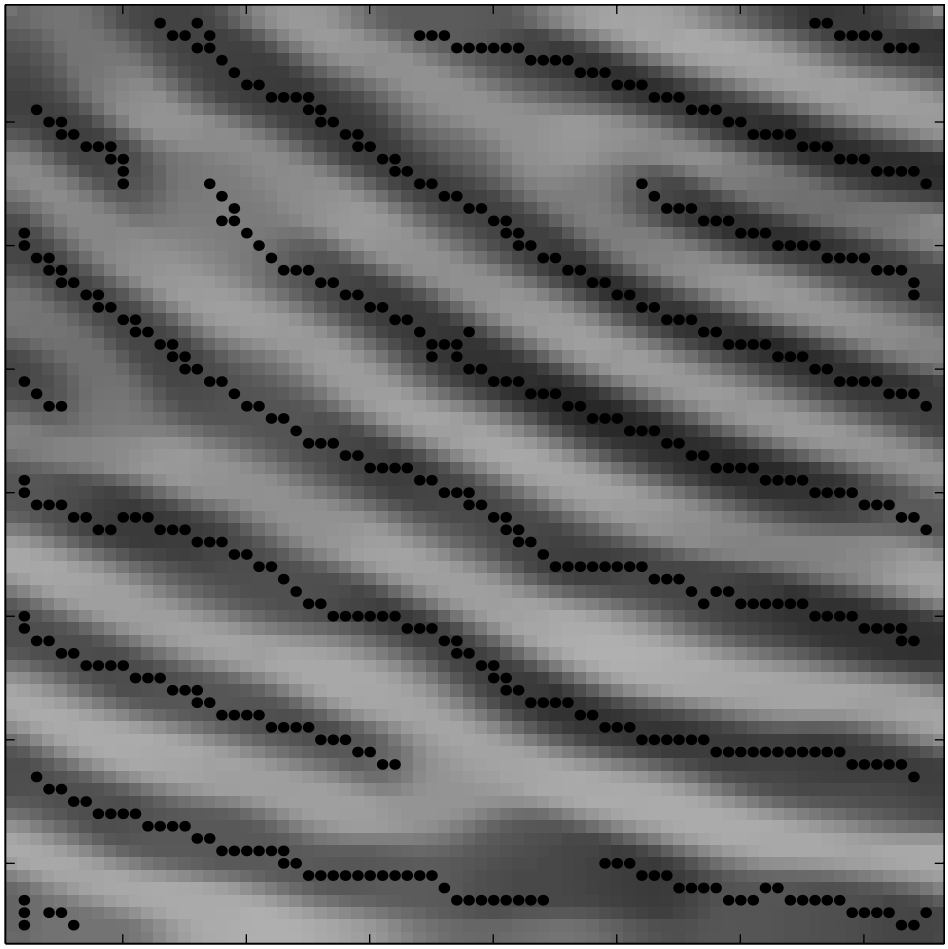

Figure 4.1: Ridge reconstruction result on a clean fingerprint area. 20 points are used, when performing *mse* line fitting, and 4 pixels is the distance recovered along the tangent direction given by the *mse* line fitting.

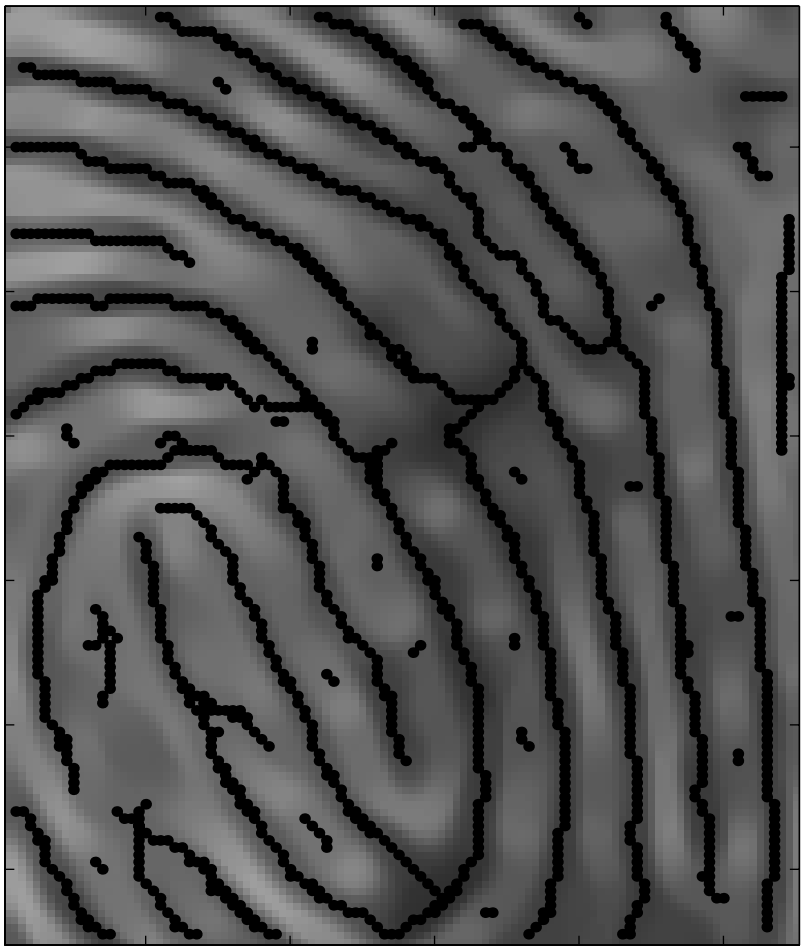

Figure 4.2: Ridge reconstruction result on a noisy fingerprint area. 10 points are used, when performing *mse* line fitting, and 6 pixels is the distance recovered along the tangent direction given by the *mse* line fitting.

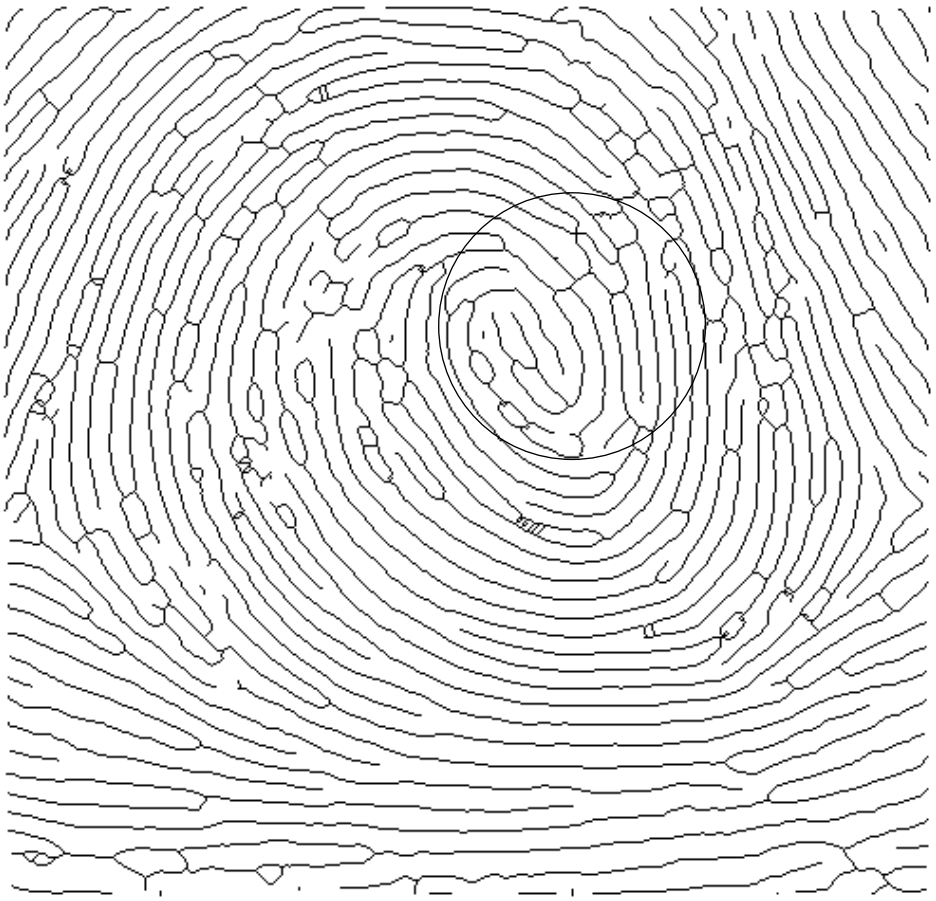

Figure 4.3: Skeleton of image shown in Figure 3.5, obtained performing binarization as explained in §2.2.

Figure 4.4: Original fingerprint image classified as poor quality image.

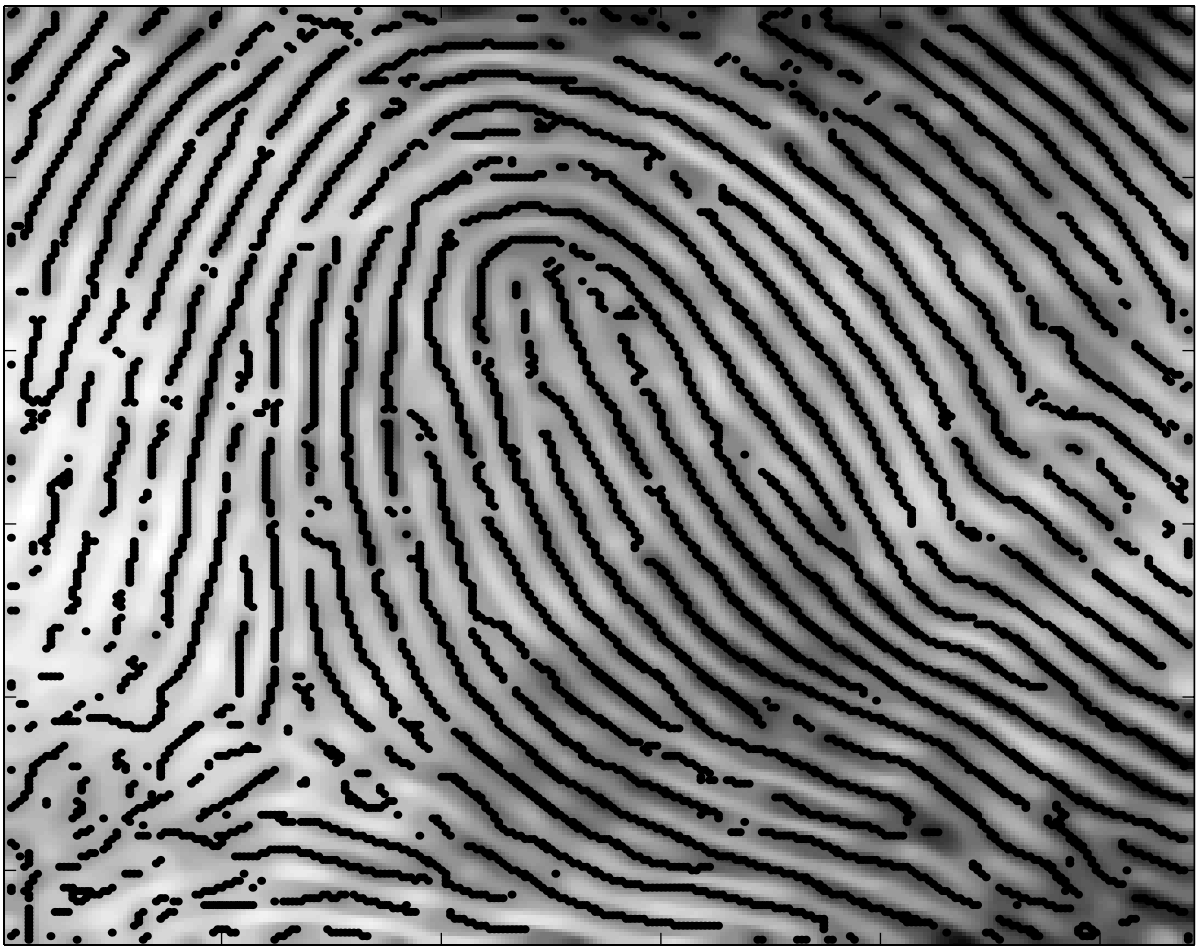

Figure 4.5: Result of ridge point detection on a whole fingerprint image. All points are shown as black dots.

Figure 4.6: Result of ridge reconstruction on a whole fingerprint image.

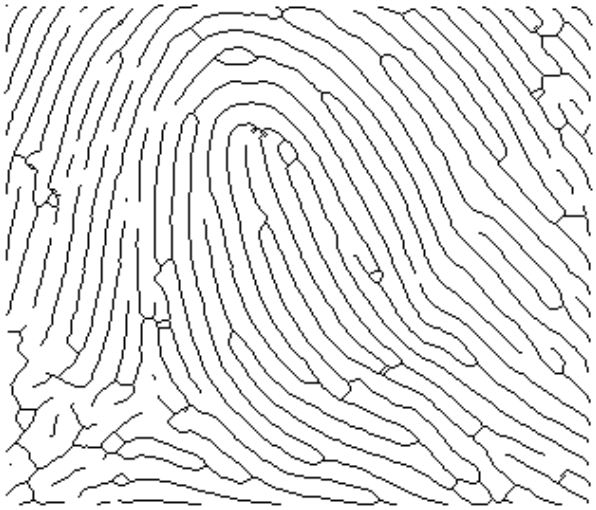

Figure 4.7: Skeleton of image shown in Figure 4.4, obtained performing binarization as explained in §2.2.

Chapter 5

Conclusions and Future Work

The ridge point detection technique and the ridge reconstruction algorithm we discussed allow us to obtain a compact fingerprint representation which retains the discriminating features of each fingerprint. The resulting structures can be directly used to address the print-to-print matching problem. In this chapter we discuss two possible alternatives to solve this problem. We also discuss a different technique to detect non stationary points on ridges, based on detection of curvature extrema points of the level curves of the gray scale images [10]. The resulting *vertex curves* should mark the branches of ridges with positive and negative slope, allowing us to fill the gaps between maximum and saddle points, without need of investigating on the angles between neighbor gradient vectors.

5.1 How to Address the Print-to-Print Matching Problem

5.1.1 Detection of Minutiae Points

For the print-to-print matching problem, bifurcation and end points extraction can easily be automatically performed directly on the image resulting from our ridge reconstruction algorithm. End points are points which have only one neighbor, whereas bifurcation points are points which have three neighbors.

A post processing stage can eliminate spurious feature points, which may be still present, based on the structural and spatial relationships of the minutiae. For instance, two minutiae in a real fingerprint cannot occur within a distance of few pixels from each other. Proper heuristics can be implemented to perform ridge break and spike elimination [21]. Two end points with the same orientation and within a distance threshold can be eliminated; an end point which is connected to a bifurcation point and is also within a distance threshold can be eliminated.

5.1.2 Template Matching

The resulting ridge structures form a template which carries information, such as curvature of ridges, length of ridges, spatial frequencies, orientation, which may be used to address the print-to-print matching problem, directly without performing feature point extraction.

The detected ridge points themselves form a template, which may be directly used to perform matching of latent fingerprints.

5.1.3 Other Extensions

One interesting direction for future research is to generate fingerprint representations which are normalized with respect to scale and rotation, using Gabor wavelets [20, 6]. Such representations would allow to avoid rotating the fingerprint images and trying to matching among all possible orientations in print-to-print match. They should significantly speed up the print-to-print matching process. The cost is more computation to generate representations that are normalized with respect to scale and rotation. However, these computations are affordable since they are off-line.
Future work will investigate if wavelet analysis can be directly applied on the representation we get from ridge point detection and ridge reconstruction, or it should be performed after minutiae point extraction.

5.2 Curvature Extrema Points

In §3.5 we describe a technique to detect non stationary points on ridges. An alternative approach to find points at the top of ridges with negative or positive slope is to identify the curvature extrema of the level curves of the image.

A gray scale fingerprint image can be seen as a smooth collection of level curves. Curvature extrema points, also called *vertex points*, are adjacent from level to level and form continuous curves on the image surface, called *vertex curves*, that mark the tops of ridges (as well as bottoms of valleys). Locating vertex curves at the top of ridges should allow us to identify fingerprint ridges towards endings and, in general, branches with positive or negative slope.

One way to calculate the exact locations of the curvature extrema is to find the zeros of the directional derivatives of level curve curvature, whose expression is given

by:

$$\frac{\partial \kappa}{\partial s} = (\kappa_x, \kappa_y)\vec{s}(x,y)^t = 0$$

where $\kappa(x,y)$ is the level curve curvature at point (x,y) and $\vec{s}(x,y)$ is the level curve tangent vector, e.g. the unit vector that is orthogonal to the level curve normal (I is the gray scale image):

$$\vec{s}(x,y) = (-I_y(x,y), I_x(x,y))/||(I_x(x,y), I_y(x,y))||.$$

The expression for the level curve curvature is:

$$\kappa(x,y) = -\vec{s}(x,y)[Hessian(I)]\vec{s}(x,y)^t.$$

The zeros of the curvature derivative function also identify vertex curves of negative curvature maxima and positive curvature minima which do not correspond to ridge tops or valley bottoms. Development of robust criteria to properly select the vertex curves which identify ridge tops will be investigated.

Bibliography

[1] Alvarez, L., Lions, P.L., and Morel J.M., 1991, "Image Selective Smoothing and Edge Detection by Nonlinear Diffusion", SIAM J. on Num. Anal..

[2] Arumugam, A., Radhakrishnan, T., Suen, C.Y., and Wang, P.S.P., 1993, "A Thinning Algorithm Based on the Force Between Charged Particles", *International Journal of Pattern Recognition and Artificial Intelligence*, Vol. **7**, No. 5, pp. 987–1008.

[3] Ballard, D.H., and Brown, C.M., 1982, "Computer Vision", Prentice-Hall, Inc..

[4] Baruch, O., October 1988, "Line Thinning by Line Following", *Pattern Recognition Letters*, Vol. **8**, No. 4, pp. 271–276.

[5] Coetzee, L., and Botha, E.C., 1993, "Fingerprint Recognition in Low Quality Images", *Pattern Recognition*, Vol. **26**, No. 10, pp. 1441–1460.

[6] Daugman, J.G., July 1988, "Complete Discrete 2-D Gabor Transforms by Neural Networks for Image Analysis and Compression", *IEEE Trans. on Acoustics, Speech, and Signal Processing*, Vol. **36**, No. 7, pp. 1169–1179.

[7] U.S. Dept. of Justice, The Science of Fingerprint, 1984, Washington D.C..

[8] Donahue, M.J., and Rokhlin, S.I., 1993, "On the Use of Level Curves in Image Analysis", *Image Understanding*, Vol. **57**, No. 2, pp. 185–203.

[9] Duda, R.O., and Hart P.E., 1973, "Pattern Classification and Scene Analysis", Wiley-Interscience Publication.

[10] Gauch, J.M., and Pizer, S.M., 1993, "Multiresolution Analysis of Ridges and Valleys in Grey-Scale Images", *IEEE Trans. on Pattern Analysis and Machine Intelligence*, Vol. **15**, No. 6, pp. 635–646.

[11] Gonzalez, R.C., and Woods R.E., 1992, "Digital Image Processing", Addison-Wesley Publishing Company.

[12] Hu, G., and Li, Z.N., 1993, "An X-Crossing Preserving Skeletonization Algorithm", *International Journal of Pattern Recognition and Artificial Intelligence*, Vol. **7**, No. 5, pp. 1031–1053.

[13] Karu, K., and Jain, A.K., 1996, "Fingerprint Classification", *Pattern Recognition*, Vol. **29**, No. 3, pp. 389–404.

[14] Langley, R.J., 1995, "An Introduction to Automated Fingerprint Identification Systems", *Technology Review, TRW Systems Integration Group*, Vol. **3**, No. 2, pp. 3–27.

[15] Lee, H.C., and Gaensslen, R.E., 1991, "Advances in Fingerprint Technology", Elsevier.

[16] Maintz, J.B.A., van den Elsen, P.A., and Viergever, M.A., 1996, "Evaluation of ridge Seeking Operators for Multimodality Medical Image Matching", *IEEE*

Trans. on Pattern Analysis and Machine Intelligence, Vol. **18**, No. 4, pp. 353–364.

[17] Moayer, B., and Fu, K., 1986, "A Tree System Approach for Fingerprint Pattern Recognition", *IEEE Trans. on Pattern Analysis and Machine Intelligence*, Vol. **8**, No. 3, pp. 376–388.

[18] Morel, J.M., and Solimini, S., 1995, "Variational Methods in Image Segmentation", Birkhäuser.

[19] O'Gorman, L., and Nickerson, J.V., 1989, "An Approach to fingerprint Filter Design", *Pattern Recognition*, Vol. **22**, No. 1, pp. 29–38.

[20] Porat, M., and Zeevi, Y.Y. , July 1988, "The Generalized Gabor Scheme of Image Representation in Biological and Machine Vision", *IEEE Trans. on Pattern Analysis and Machine Intelligence*, Vol. **10**, No. 4, pp. 452–468.

[21] Ratha, N.K., Chen, S., and Jain, A.K., 1995, "Adaptive Flow Orientation-Based Feature Extraction in Fingerprint Images", *Pattern Recognition*, Vol. **28**, No. 11, pp. 1657–1672.

[22] Ratha, N.K., Karu, K., N.K., Chen, S., and Jain, A.K., 1996, "A Real-Time Matching System for Large Fingerprint Databases", *IEEE Trans. on Pattern Analysis and Machine Intelligence*, Vol. **18**, No. 8, pp. 799–813.

[23] Shah, J., 1996, "A Common Framework for Curve evolution, Segmentation, and Anisotropic Diffusion", *CVPR 96.*

[24] Stock, R.M., and Swonger, C.W., 1969, "Development and Evaluation of a Reader of Fingerprint Minutiae", Cornell Aeronautical Laboratory, Technical Report CAL No. XM-2478-X-1:13-17.

[25] Suzuki, S., Ueda, N., and Sklansky, J., 1993, "Graph-Based Thinning for Binary Images", *International Journal of Pattern Recognition and Artificial Intelligence*, Vol. **7**, No. 5, pp. 1009–1030.

[26] Verma, M.R., Majumdar, A.K., and Chatterjee, B., 1987, "Edge Detection in Fingerprints", *Pattern Recognition*, Vol. **20**, No. 5, pp. 513–523.

[27] Watson, C.I., and Wilson, C.L., March 1992, NIST Special Database 4, Fingerprint Database, National Institute of Standards and Technology.

[28] Watson, C.I., May 1993, NIST Special Database 9, Fingerprint Database, National Institute of Standards and Technology.

[29] Watson, C.I., September 1993, NIST Special Database 14, Fingerprint Database, National Institute of Standards and Technology.